CRRES/MEA and CRRES/HEEF Electrons

This document discusses development of data sets of energetic electron observations from the Medium Electron Sensor A (MEA) and High Energy Electron Fluxmeter (HEEF) instruments on the CRRES satellite. Since intercalibration of these two data sets was performed in conjunction with data processing and cleaning, the two data sets are described together. Processing of the data sets included cleaning for proton contaminated MEA data and MEA/HEEF data with incomplete pitch angle data, spectral correction of MEA data, and adjustment of HEEF data at high flux levels.

1. Spacecraft

The Combined Release and Radiation Effects Satellite (CRRES) was a joint AFGL/NASA/ONR mission launched on 25 July 1990 and providing data through 11 October 1991. Its orbit was 350 km x 33500 km with an inclination of 18°. The satellite maintained a Sun-pointing spin axis with a spin rate of ~2 rpm. Among its instruments for particle detection were the Medium Electron Sensor A (MEA) and the High Energy Electron Fluxmeter (HEEF), both providing observations of energetic electrons. Both instruments provided pitch-angle resolved observations, using data from the CRRES fluxgate magnetometer. For an overview of CRRES see [1].

2. Detectors

2.1. MEA instrument

The Medium Electron Sensor A (MEA) is a magnetic-focusing electron spectrometer. Electrons entering the instrument are deflected by a vertical magnetic field, curving to reach one of 17 silicon detectors depending on their energies. MEA observes electrons from 153 keV to 1.582 MeV in 17 differential channels, with an additional channel to provide background measurements. MEA field of view is 1.4-8.2° half-angle, depending on energy, allowing pitch-angle resolved observations given the spin of the CRRES spacecraft. For more information on the MEA instrument see [2].

The MEA instrument flown on CRRES was originally built as a spare for an instrument flown on OV1-19 in 1969. The MEA was subsequently modified, changing the observed energy range, and eventually recalibrated prior to launch on CRRES. Nominal mid-channel energies for the channels are given in Table 1.

Table 1. Characteristics of CRRES/MEA electron channels [3].

Channel (this doc)	Channel (Vampola)	E (keV)	E_{min} (keV)	E_{max} (keV)	dE (keV)	GEF (cm^2-sr-keV)	Half Angle (°)
1	0	148	110	188	78	5.88	8.24
2	1	214	174	257	83	5.68	6.37
3	2	272	230	314	84	5.16	5.19
4	3	341	297	384	87	4.84	4.38
5	4	417	374	462	88	4.59	3.78
6	5	509	465	553	88	4.19	3.24
7	6	604	558	649	91	3.89	2.90
8	7	692	646	738	92	3.58	2.63
9	8	782	735	829	94	3.30	2.40
10	9	876	828	923	95	3.08	2.21
11	10	976	928	1024	96	2.89	2.05
12	11	1090	1042	1139	97	2.66	1.88
13	12	1178	1131	1227	96	2.49	1.76
14	13	1288	1239	1337	98	2.37	1.66
15	14	1368	1322	1419	97	2.23	1.56
16	15	1472	1423	1520	97	2.14	1.48
17	17	1582	1534	1633	99	2.03	1.41

2.2. HEEF instrument

The AFGL High Energy Electron Fluxmeter (HEEF) comprises two solid state detectors (SSDs) and a bismuth germinate (BGO) crystal scintillator with the latter surrounded by an anti-coincidence plastic scintillator. Normally a triple coincidence in the two SSDs and BGO accompanied by anti-coincidence in the plastic scintillator indicates a particle detection, with the energy deposition signature in the SSDs and BGO used to determine particle energy and species (i.e. electron or proton). HEEF observes electrons with energies from 0.6 to 8 MeV. HEEF field of view is ~12° half-angle, accommodating pitch angle-resolved observations given spinning of the CRRES spacecraft. For more information on the HEEF instrument see [4].

The HEEF instrument was extensively calibrated prior to launch. Shortly after launch it was necessary to turn off a heater in the HEEF compartment, with the result that HEEF operating temperatures were significantly different than planned. Since the BGO operation is temperature sensitive, further calibration work on HEEF was completed using on-orbit data and laboratory calibration of a spare unit. In addition, HEEF observations were compared with CRRES Dosimeter observations. Extensive descriptions of both pre- and post-launch calibrations are available [5][6]. Ten differential and eight integral energy channels are defined, but the lowest differential energy channel is unreliable and is not used. Two additional differential channels (0.65 and 0.95 MeV) are derived from differencing pairs of integral channels. Nominal mid-channel energies for the differential channels are given in table 2.

Table 2. Characteristics of CRRES/HEEF electron channels [6].

Channel (this doc)	Channel (Hanser)	E (MeV)	GEF, T=0° C (cm^2-sr-keV)	E, T=0° C (MeV)	GEF, T=-10° C (cm^2-sr-keV)	E, T=-10° C (MeV)
0		0.65				
1		0.95				
2	L1	1.60	0.1151	1.52	0.0381	1.45
3	L2	2.00	0.230	1.96	0.0690	1.85
4	L3	2.35	0.295	2.36	0.0802	2.23
5	L4	2.75	0.395	2.79	0.0957	2.63
6	L5	3.15	0.448	3.23	0.0975	3.06
7	L6	3.75	1.065	3.80	0.1981	3.59
8	L7	4.55	1.302	4.65	0.1992	4.39
9	L8	5.75	2.410	5.83	0.2780	5.48
10	L9	7.50	2.400	7.57	0.1949	7.13

2.3. Prior data sets

AFRL (formerly AFGL) has released versions of the HEEF and MEA data sets. The MEA data set includes dead-time/foldover and background corrections and was posted to the NASA Space Science Data Center (NSSDC) in September 2000 [3]. This set was at the 0.512-s instrument resolution but was later processed into one minute averages and posted at Goddard Space Flight Center's CDAWeb in May 2003. The HEEF data set provides one minute averages and includes temperature corrections (addressing the temperature-dependent BGO sensitivity) and dead-time corrections (both described in [6]) and was posted to the NSSDC in October 2001 [7]. Other versions of these data sets exist, e.g. the MEA data set processed for TREND [8].

3. Data Processing

Starting from the AFRL data sets, we completed a reanalysis and cross-calibration of the two data sets, utilizing the overlap between the MEA and HEEF instruments with channels at 1.6 MeV (these channels are referred to hereafter as MEA-17 and HEEF-2, respectively). Primarily, this data set applied the following data cleaning and corrections to the AFRL MEA/HEEF data sets:

- Removal of proton-contaminated data
- Removal of data missing too many individual pitch-angle values
- Correction of MEA flux values for varying energy spectral slope
- Correction of HEEF flux values to adopt median agreement with MEA
- Merge with K/Φ/L* values

3.1. Initial data set

We started from existing AFRL-produced data sets containing one minute averages of fluxes reported in pitch angle increments of 5°. These data sets were derived from the original 0.512-s resolution data. With the spacecraft rotating at ~2 rpm and pitch angle reported over the range 0-90°, this provides ~8 points per pitch angle bin per minute. In the case of HEEF, the AFRL data set included temperature and deadtime corrections. From these we obtained omnidirectional fluxes, applying the reported fluxes uniformly for pitch angle values in each bin:

$$J = 4\pi \int_0^{\pi/2} j(\alpha)\sin(\alpha)d\alpha = 4\pi \sum_{i=1}^{19} j(\alpha)\left[\cos(\alpha_i) - \cos(\alpha_i')\right],$$

with $\alpha_i = [5(i-1)-2.5]°$, $\alpha'_i = [5(i+1)-2.5]°$ (except $\alpha_1 = 0$ and $\alpha'_{19} = 90°$). Figure 1 shows the resulting omnidirectional flux values, HEEF observations vs. MEA observations, before any current data cleaning or corrections.

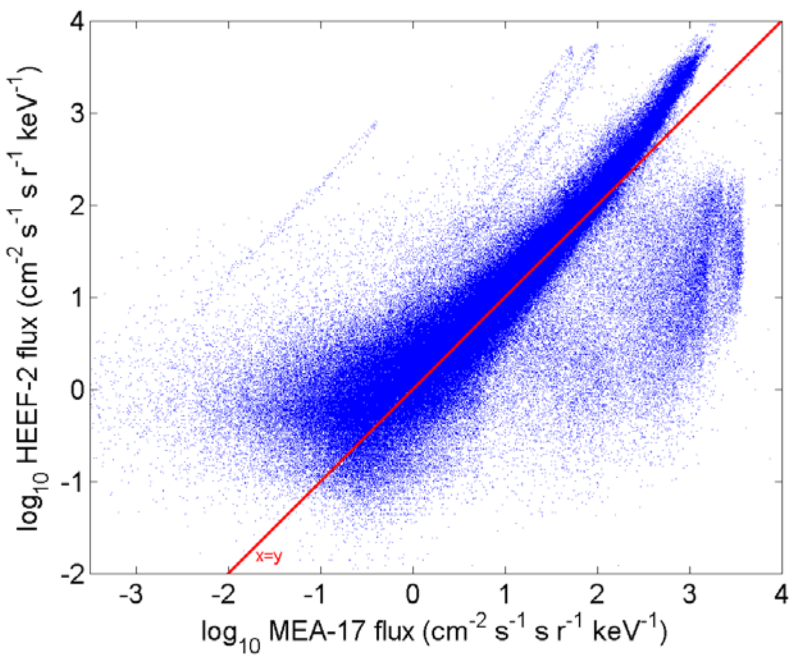

Figure 1: HEEF-2 fluxes vs. MEA-17 fluxes, original omnidirectional data (before cleaning)

3.2. Removal of proton-contaminated data

Most cases with MEA-17 flux much greater than HEEF-2 flux we conclude are due to proton contamination, based on the fact that they occur either when L<2-3, or during the most intense solar proton events of the CRRES mission period. Based on comparison of the two channels, we omit MEA data meeting any of the following criteria:

- L<2.0 and prior to day 82.0 of 1991 (inner proton belt, pre-March 1991 storm);
- L<2.9 and after day 82.0 of 1991 (inner proton belt, post-March 1991 storm);
- From day number 82.85 to 83.00 of 1991 (solar proton event);
- From day number 161.95 to 163.10 of 1991 (solar proton event).

3.3. Removal of incomplete observations

Cases with HEEF-2 flux much greater than MEA-17 flux for pitch angle averaged data also resulted from observations with missing pitch angle-resolved data. We elected to drop all flux values for observations with incomplete pitch-angle values. We adopted criteria to filter out cases where pitch angle-resolved data is significantly incomplete:

- HEEF data from day number 236.05 to 236.37;
- HEEF data where the number of zero pitch angle-resolved flux values is greater than 14, and the omnidirectional flux is greater than 10 $cm^{-2}s^{-1}sr^{-1}keV^{-1}$.
- MEA data where the highest pitch angle resolved flux is greater than 10 $cm^{-2}s^{-1}$ $sr^{-1}keV^{-1}$, but this value is greater than 10 times the omnidirectional flux value.

Relative scatter between HEEF and MEA data is greater at low flux values due to low count statistics. MEA observations tend to exhibit a noise floor around 0.1 $cm^{-2}s^{-1}$ $sr^{-1}keV^{-1}$ (corresponding to ~0.2 counts s^{-1}) whereas HEEF fluxes with value zero are reported.

3.4. Spectral corrections

Conversion of instrument counts in both MEA and HEEF is sensitive to assumptions regarding energy spectra. In the prior data sets, this conversion assumes a power law spectra $j \sim e^n$ with fixed spectral index n, n=0 for MEA [9] and n=-6 for HEEF [6] (As noted in [9], an alternate MEA data set by Bourdarie uses n=-3).

For MEA, Vampola provides channel geometric factors and nominal energies for integer values of n from -8 to 0. We adopted an algorithm to correct MEA channel fluxes as follows:

- Determine the power law spectral index for channel k by fitting to fluxes from channels k+1 and k-1 (or, for the highest and lowest energy channels, from channel k and the adjacent channel);
- Adopt the correction factor from Vampola from the closest tabulated index value;
- Iterate each energy spectra five times (note that results mostly converge on the first iteration);
- Interpolate from the corrected nominal energy back to the standard nominal energy (to provide results for a uniform set of energy values).

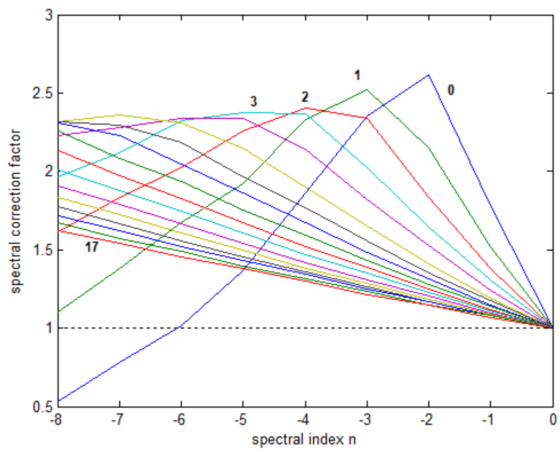

Figure 2: MEA channel spectral correction factors as functions of spectral index, with curves for several channels labeled to show the progression.

We sought to apply a similar process to HEEF data, using reported channel response functions. Figure 3 shows the measured geometric factor (GEF) and hypothetical GEF for the differential channels from [6]. Calculations based on these GEFs indicate correction factors ranging from 0.5 to 5 for spectral index values from -10 to 0 depending on the channel. Unfortunately, preliminary results showed that corrections failed to converge to a meaningful result, likely due to differences between the adopted and actual GEF functions. (Another factor is the observed complexity of electron spectra, examined during AE9/AP9 development [10]). Note that the GEF for HEEF channels is temperature dependent, due to the previously mentioned issue with the BGO scintillator. Spectral correction/inversion of the HEEF data would require improved estimates of channel GEFs which was beyond the scope of the current investigation. Consequently we retain the existing spectral assumptions in the HEEF data set, i.e. power-law form with n=-6.

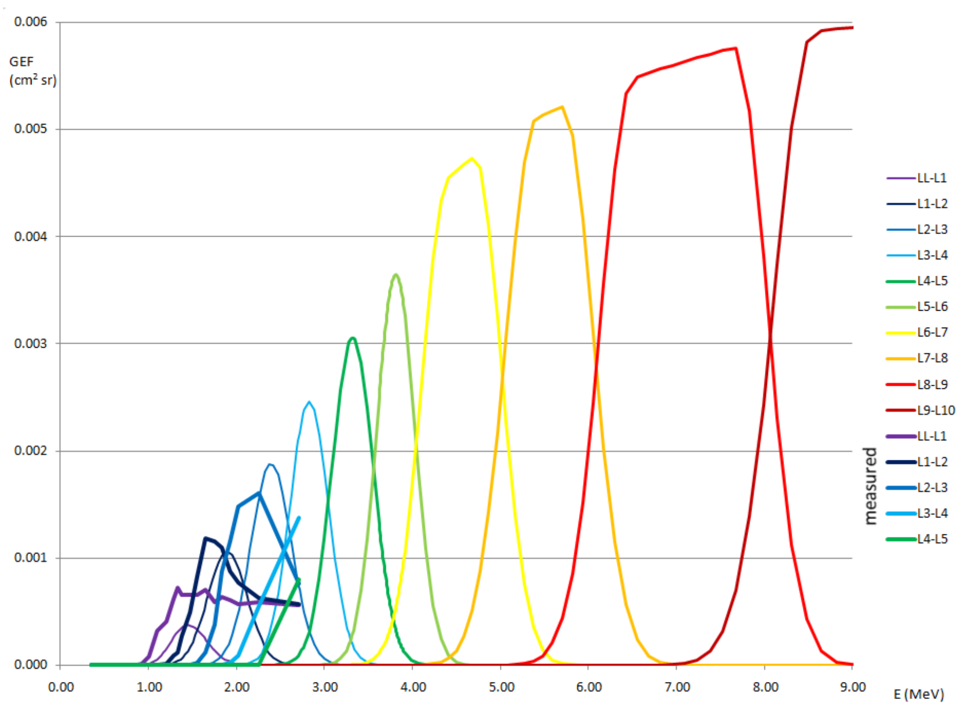

Figure 3: HEEF channel GEF(E), measured (thick lines) up to E=2.8 MeV, and hypothetical (thin lines).

3.5. Cross-calibration of MEA and HEEF data

Figures 4 and 5 illustrate the improved agreement between MEA and HEEF following the data cleaning and MEA spectral correction as described above. There remains, however, a significant disagreement between MEA and HEEF at high flux levels, ranging from near agreement at fluxes ~10^2 $cm^{-2}s^{-1}sr^{-1}keV^{-1}$ and increasing to a factor of 3 higher flux in HEEF when MEA-17 observes fluxes ~10^3 $cm^{-2}s^{-1}sr^{-1}keV^{-1}$.

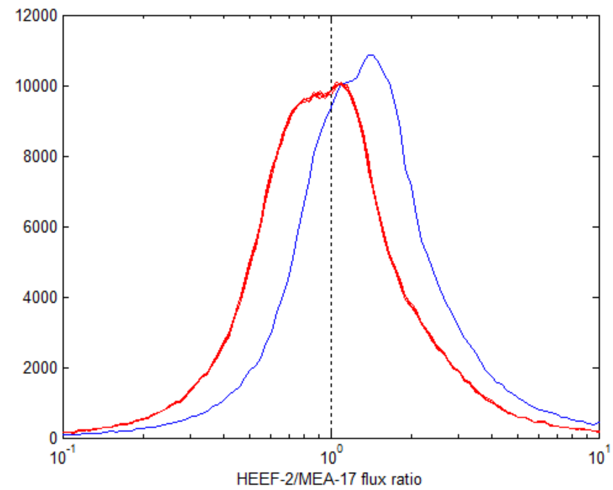

Figure 4: Histogram of HEEF-2/MEA-17 flux ratio values, uncorrected (blue) and after data cleaning and MEA spectral correction (red).

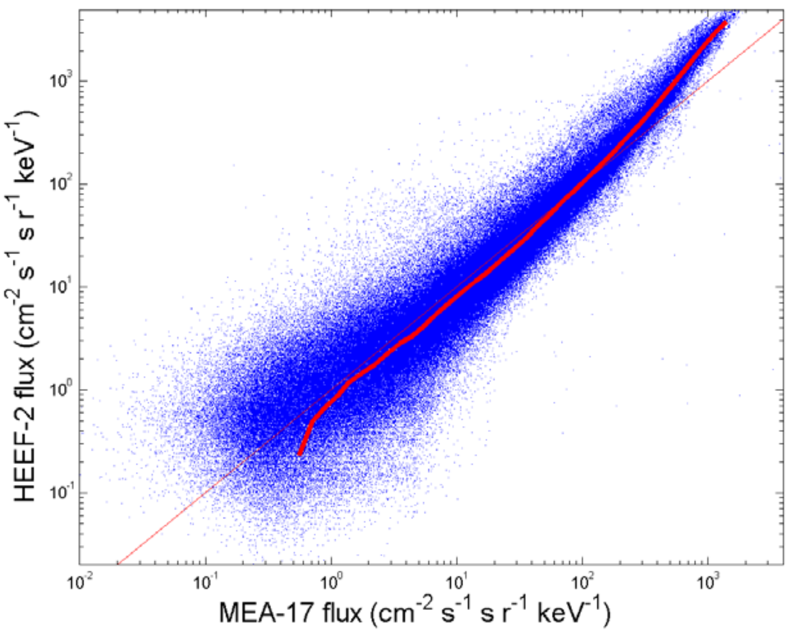

Figure 5: HEEF-2 vs. MEA-17 flux values, after data cleaning and MEA spectral correction. Thick red line shows median trend with MEA flux.

Our investigation suggests that this may result from the deadtime correction in the HEEF data set. Based on this, we adopted the MEA observations as standard and used an empirical correction factor as a function of the MEA-17 flux value. Figure 6 shows this correction as a function of flux observed in the HEEF-2 (1.6 MeV) channel. Based on the hypothesis that this is an issue with the deadtime correction, this correction factor based on channel 2 is also applied identically to the simultaneous observations in channels 3-10. However, this issue could be revisited.

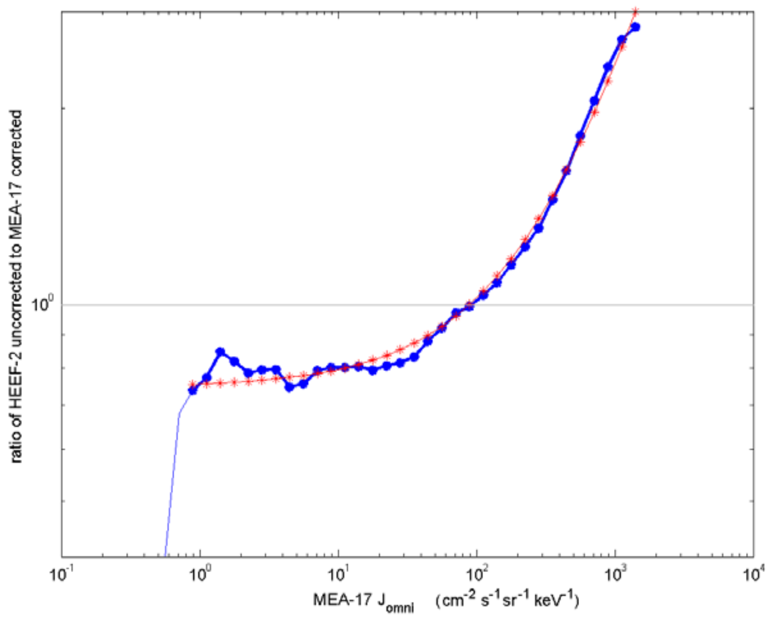

Figure 6: Median HEEF-2/MEA-17 flux ratio as a function of MEA-17 flux (blue), and adopted empirical correction factor (red).

Figure 7 illustrates the final results by plotting HEEF-2 fluxes vs. MEA-17 fluxes for the data set after all data cleaning and corrections.

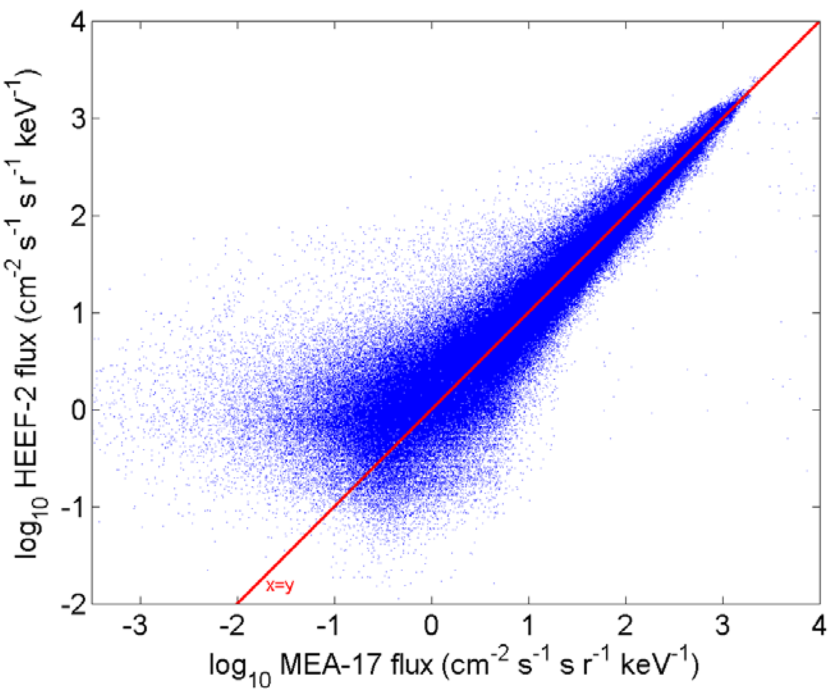

Figure 7: HEEF-2 vs. MEA-17 fluxes, omnidirectional, final data set.

MEA and HEEF data for $h_{min} \leq 1100$ km was not used in AE9.

4. Conclusion

Versions of the MEA and HEEF data sets as processed for AE9/AP9 are publicly available at the ViRBO web site [10].

5. References

[1] Gussenhoven, M. S., E. G. Mullen, and D. H. Brautigam (1996), Improved understanding of the Earth's radiation belts from the CRRES satellite, *IEEE Trans. Nucl. Sci.*, 43(2):353-368.

[2] Vampola, A. L., J. V. Osborne, and B. M. Johnson (1992), The CRRES magnetic electron spectrometer AFGL 701-5A (MEA), *J. Spacecr. Rockets*, 29:592-594.

[3] Vampola, A. L. (2000), "0.5-second electron spectra at 0.1-2 MeV from the CRRES MEA Magnetic Spectrometer," NSSDC Data Set SPMS-00233, *NSSDC*, on line [http://nssdc.gsfc.nasa.gov/nmc/datasetDisplay.do?id=SPMS-00233].

[4] Dichter, B. K., and F. A. Hanser (1992), *Development and Use of Data Analysis Procedures for the CRRES Payloads AFGL-701-2/Dosimeter and AGRL-701-4/Fluxmeter and Application of the Data Analysis Results to Improve the Static and Dynamic Models of the Earth's Radiation Belts*, PL-TR-92-2223, Phillips Laboratory, AFMC, Hanscom AFB, MA.

[5] Dichter, B. K., F. A. Hanser, B. Sellers, and J. L. Hunerwadel (1993), High Energy Electron Fluxmeter, *IEEE Trans. Nucl. Sci.*, 40(2):242-245.

[6] Hanser, F. A. (1995), *Analyze Data from CRRES Payloads AFGL-701/Dosimeter and AFGL-701-4/Fluxmeter*, PL-TR-95-2103, Phillips Laboratory, AFMC, Hanscom AFB, MA.

[7] Brautigam, D. (2001), *Combined Release and Radiation Effects Satellite (CRRES) High Energy Electron Fluxmeter (HEEF) and Proton Telescope (PROTEL)*, AFRL, Hanscom AFB, MA, previously on line at *NSSDC* [ftp://nssdcftp.gsfc.nasa.gov/ spacecraft_data/crres/particle_heef/document/crres_readme3.pdf].

[8] Lemaire, J., D. Heynderickx, A. D. Johnstone, E. Keppler, M. Kruglanski, D. J. Rodgers, G. Jones, S. Szita, R. Friedel, and G. Loidl (1998), *Trend-3 Radiation Environments of Astronomy Missions and LEO Missions Final Report*, ESA.

[9] Cayton, T. E. (2007), *Objective Comparison of CRRES MEA Electron Spectra Using Response Functions for the SOPA Aboard S/C 1989-046*, LA-UR-07-8023, LANL, Los Alamos, NM.

[10] Johnston, W. R., C. D. Lindstrom, and G. P. Ginet (2012), Characterization of radiation belt electron energy spectra from CRRES observations, in preparation.

[11] Johnston, W. R., C. D. Lindstrom, and G. P. Ginet (2011), CRRES Medium Electron Sensor A (MEA) and High Energy Electron Fluxmeter (HEEF): Cross-calibrated data set, AFRL, available at *ViRBO* [ftp://virbo.org/johnston/crres/ MEAHEEFCC.pdf].

TSX5/CEASE Electrons

This document provides a brief discussion of how the TSX5/CEASE electron flux data set used in AE9 was generated. It includes brief descriptions of the detectors used, their response to ambient electron fluxes, instrument calibration, data analysis, and data cleaning. Detailed descriptions of each of these aspects will be provided elsewhere.

1. Spacecraft

TSX5 was a small USAF spacecraft placed in a 404 km x 104 km x 69 deg orbit. Data were taken from 2000-06-06 until 2006-07-05, a total of 6.1 years; this period started near the maximum of solar cycle 23 and ended near solar minimum. The nominal data sampling rate was 5 seconds.

2. Detector

The CEASE I instrument consists of a two element telescope detector and two dosimeter-type detectors as well as a single event sensor [1]. The initial data processing consisted of unpacking the raw telemetry, applying dead time corrections, and summing appropriate raw channels to create standard channels as described in reference [2]. Data processing for AE9 v1.0 used three standard channels from the dosimeter and four from the telescope. Table 1 lists the energy thresholds and geometric factors for the channels to electrons. The following subsections discuss these parameters in more detail. As can be seen from this table CEASE responds to electrons nominally between 100 keV-3 MeV.

Table 1. Characteristics of TSX-5/CEASE electron channels

Channel	Type	Eth MeV	G cm^2 sr	FOV Degrees	BG cts/sec
D01	Dosimeter	1.23	0.354	160	0.65
D02	Dosimeter	2.42	0.0659	160	0.65
D03	Dosimeter	1.65	0.0301	160	0.11
T01	Telescope	0.11	9.86e-4	45	0.77
T02	Telescope	0.15	7.81e-4	45	0.42
T03	Telescope	0.35	4.70e-4	45	0.2
T04	Telescope	0.57	2.74e-4	45	0.07

NOTE: E_{th}, G determined by modified bow-tie analysis in AFRL-VS-HA-TR-2008-1129.

2.1. Response Functions

The CEASE standard channels respond to a rather broad range of energies and to both protons and electrons. Monte-Carlo simulations of the detector geometry were used to determine energy- and angle-dependent response functions for each channel for both protons and electrons; these are documented in Reference [3]. Reference [1] also derived approximate threshold energies and geometric factors for the channels; these are the parameters listed in Table 1. Because of the structure of the energy-dependent response function, these parameters are only crude representations of the instrument response; in reality, the threshold energy and geometric factor are strongly dependent on the spectral shape. This can be seen in figure 1 which shows the energy dependent response for telescope channel T01 to both electrons and protons. For this reason, a more sophisticated spectral inversion technique was used to derive fluxes from the data.

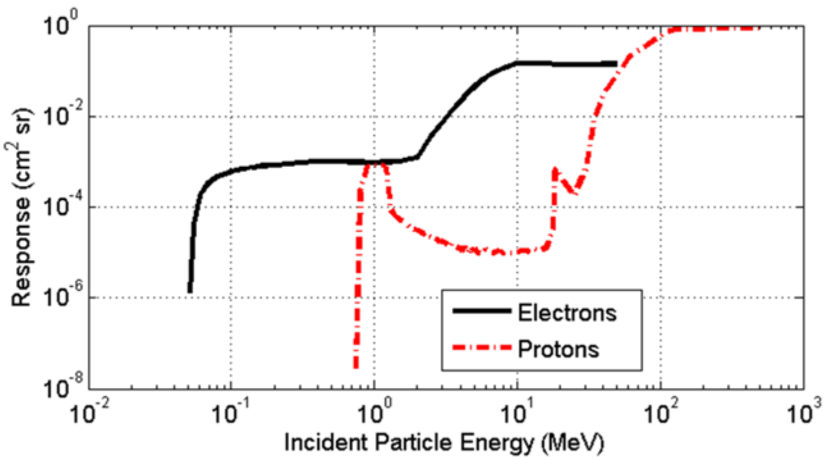

Figure 1. Response of channel T01 to isotropic fluxes of protons and electrons

2.2 Background Determination

Background count rates were determined by averaging counts in each channel in regions outside the nominal radiation belts. The resulting background is given in Table 1.

3. Data Processing

This section briefly describes the procedures to go from count rates to the calibrated differential directional fluxes used to develop AE9. The details of these procedures will be documented elsewhere.

3.1. Spectral Inversion

The CEASE channels respond to the incident particle flux through equation 1 which shows how the response function of a CEASE channel is convolved with the incident particle flux in both angle and energy. This equation shows how the count rate in the i'th channel, C_i, are related to the energy dependent effective area of the channel, A_i, and the incident differential particle flux, j^k, for the k'th particle type (i.e. proton, electron, alpha, etc.).

$$C_i(\mathbf{x},t) = \sum_{k=1}^{\#Types} \int_0^{\infty} dE \int_0^{2\pi} d\phi' \int_0^{\pi} d\theta' \sin(\theta') A_i^k(E,\theta') j^k(E,\theta,\varphi,\mathbf{x},t) \approx$$

$$\int_0^{\infty} \hat{j}_{el}(E,\mathbf{x},t) R_i^{el}(E,\mathbf{x},t) dE + C_{back} \qquad (1)$$

To obtain the differential fluxes required for AE9, an approximate solution to this integral equation was used. This was done in a two step process by first solving equation 1 by making the approximation that the incident flux was isotropic and only due to electrons plus the small background. The assumption that the count rate was being driven only by incident electrons was verified during data processing by using proton channel D05 as a veto. If this channel exceeded 4 counts in a 15 second measurement interval, the inversion was not attempted and the data was removed from set used to construct AE9. This constraint effectively removed TSX-5 electron measurements from the inner zone. Even with the approximations in equation 1, it represents a severely undetermined system with only the seven channels of table 1. A standard approach to this problem is to approximate the spectrum as a power law or exponential function of the incident particle energy. However, the deficiencies of such an approach are well known from higher precision measurements of electron spectra in the radiation belts from such missions as CRRES as shown in figure 2.

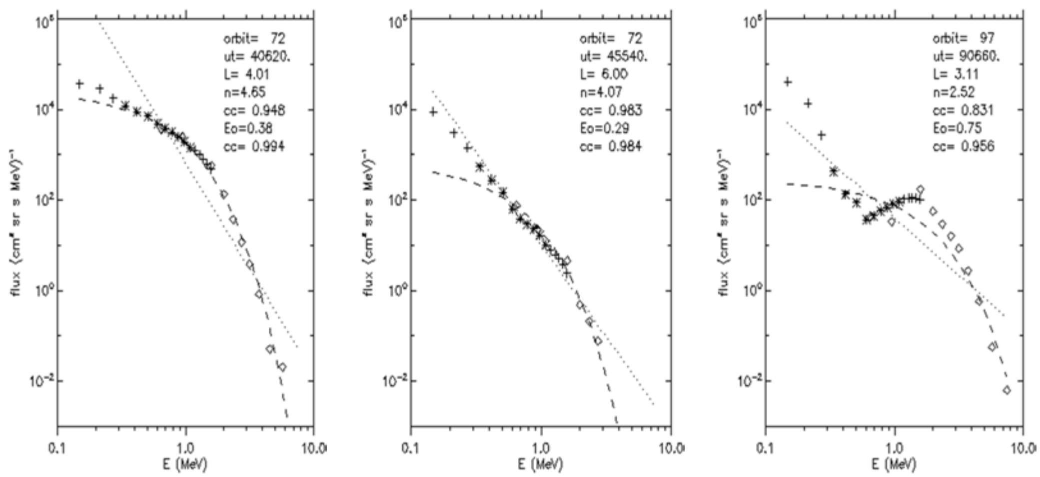

Figure 2. Examples of three different electron spectral shapes from CRRES

To deal with the multiple spectral shapes that are evident in high precision radiation belt electron measurements, a new method of spectral inversion based on principal components analysis was used. As applied to electron data sets in AE9, combined MEA and HEEF spectra were subdivided into the following seven regions:

(1) $L_m <= 2.5$
(2) $2.5 < L_m <= L_m$ value of 5 day plasmapause minimum [5ppmin]
(3) 5ppmin$<L_m<=$5ppmin+1
(4) 5ppmin+1$<L_m<=$5ppmin+2
(5) 5ppmin+2$<L_m<=$5ppmin+3
(6) 5ppmin+3$<L_m<=$5ppmin+4
(7) 5ppmin+4$<L_m$

The reason for using the 5 day plasmapause minimum as the reference is that recent work has shown a strong correlation of this location and electron spectral shape [4]. The plasmapause location was computed using the O'Brien – Moldwin model [5] parameterized by Dst but not by local time. The mean of the log (natural logarithm) electron spectral fluxes and the first ten principal components were computed for each region. The eigenvalues for the principal components are used to give *a priori* estimates of the importance of each principal component during the inversion process and are used to regularize the solution to the integral equation. Details of the actual inversion algorithm and its performance will be provided elsewhere.

For each 15 second TSX-5 measurement, a spectral inversion was then performed using the appropriate basis set based on what the L_m value was during the time of the measurement. The resulting spectral shape was then determined from the model coefficients and basis functions by equation 2:

$$j(E,t) = \exp\left(\bar{x}(E) + \sum_{i=1}^{N} q_i(t) b_i(E) \right) = \mu(E) \prod_{i=1}^{N} B_i(E)^{q_i(t)} \qquad (2)$$

where j(E,t) is the differential flux at time t, μ(E) is the mean flux, $B_i(E)$ is the i'th basis function, and $q_i(t)$ is the i'th coefficient.

During the data processing, the entire TSX5/CEASE data set was spectrally inverted at 15-second time resolution which was generated from the native 5 second resolution by averaging. At this time the data were also merged with adiabatic invariant data (e.g., K, Φ, L_m, etc.) which were calculated separately from the spacecraft ephemeris.

In addition to the energy inversion, an angular correction factor was applied to account for the wide field of view of the detector and the anisotropic nature of the electron flux. The particular model that was used to correct for angle was a $\sin^n$ model where the power indices came from Vampola's analysis of the CRRES data set [6]. The correction accounted for the look direction of the detector relative to the magnetic field line, as well as the angular response of each detector channel. The angular correction factor ξ typically ranged from 2 to 5; in some cases, however, "bad" values were obtained when conditions were outside the range of validity of the pitch angle distribution model. We expect that future releases of AP9 will include an improved pitch angle model and a combined spectral-angular inversion.

3.2. Data Cleaning

The purpose of data cleaning is to identify and eliminate data points with obvious contamination or other problems which would make the data inaccurate. Data cleaning for TSX5/CEASE electrons included the following procedures:

- As previously mentioned the D05 proton channel for CEASE was monitored and used to veto measurements that would be proton contaminated. This primarily removed points in the inner zone.
- An SPE flag based on GOES proton data was used to remove data during solar proton events

- Time-offset scatter plots. These plots would ordinarily reveal anomalous spikes in the time series data. Virtually no spikes were identified, but a filter was implemented to catch the few spikes that existed.
- Count histograms. These plots can identify potential pile-up or dead-time issues; none were found.

4. References

[1] Dichter, B.K., et al., "Compact Environmental Anomaly Sensor (CEASE): A Novel Spacecraft Instrument for *In Situ* Measurements of Environmental Conditions", *IEEE Trans. On Nuclear Science*, vol. 45, No.6, December 1998.

[2] Brautigam, D. H., "Compact Environmental Anomaly Sensor (CEASE): Geometric Factors", AFRL-VS-HA-TR-2008-1129, November 2008.

[3] Brautigam, D. H., "Compact Environmental Anomaly Sensor (CEASE): Response Functions", AFRL-VS-HA-TR-2006-1030, March 2006.

[4] Johnston, W. R., C. D. Lindstrom, and G. P. Ginet (2012), Characterization of radiation belt electron energy spectra from CRRES observations, in preparation.

[5] O'Brien, T. P., and M. B. Moldwin (2003), Empirical plasmapause models from magnetic indices, *Geophys. Res. Lett.*, 30(4):1152-1155, doi:10.1029/2002GL016007.

HEO-1/Dosimeter Electrons

1. Spacecraft

The HEO-1 satellite is in a highly elliptical orbit with period of about 12 hours, perigee of about 500 km, apogee of about 39000 km, and inclination of about 63°. This type of orbit covers the inner zone, slot region and the outer zone of the radiation belts. Data used for AE9 covered from May 1994 to February 2011, although available data coverage is intermittent.

2. Detector

The satellite database of flux data consist of energetic particle measurements, which are 15-second averages of particle data collected in 1-second integration intervals from the various on-board sensors.

Table 1. Characteristics of HEO-1/DOS channels

Channel	E (MeV)	G (cm^2 sr)	Cosmic Ray BG (cts/sec)	Proton Background (channel & coefficient)
E3/Elec3	>1.5	0.47	0.010	2.76*Prot4
E4/Elec4	>4.0	0.47	0.015	2.32*Prot5
E5/Elec5	>6.5	0.49	0.012	2.88*Prot6
E6/Elec6	>8.5	0.49	0.012	2.98*Prot7

2.1. Response Functions

The HEO-1/DOS channels respond to a rather broad range of energies starting at approximately the threshold level. Because of this, calibrated channel responses were used as a function of incident particle energy in the spectral inversion algorithm. A sample plot for Elec3 is shown in figure 1.

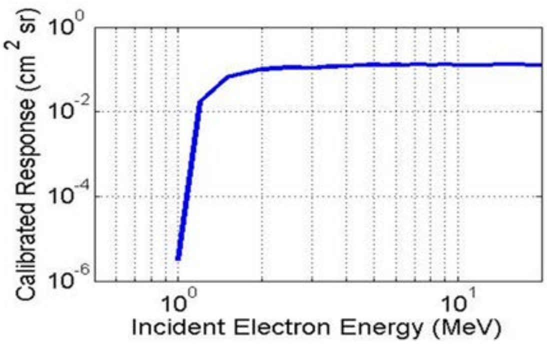

Figure 1. Response of channel Elec3 to isotropic fluxes of electrons

2.3 Background Determination

Background count rates were determined by averaging counts in each channel in regions outside the nominal radiation belts. The proton background coefficients for each electron channel were estimated from scatter plots of the electron versus proton channels as shown in figure 2. The resulting background is given in Table 1.

3. Data Processing

This section briefly describes the procedures to go from count rates to the calibrated differential directional fluxes used to develop AE9. The details of these procedures will be documented elsewhere.

3.1. Data Formatting and Filtering

The data was first summed into 0.1 wide L-bins for each orbit before performing the subsequent filtering and inversion steps. The background counts were then determined for each L-bin interval and the proton background was estimated using the appropriate proton channel and coefficient. If the count rates in each channel were higher than the background and no solar proton event was present during the period of measurement then a spectral inversion similar to the CEASE TSX-5 instrument was performed.

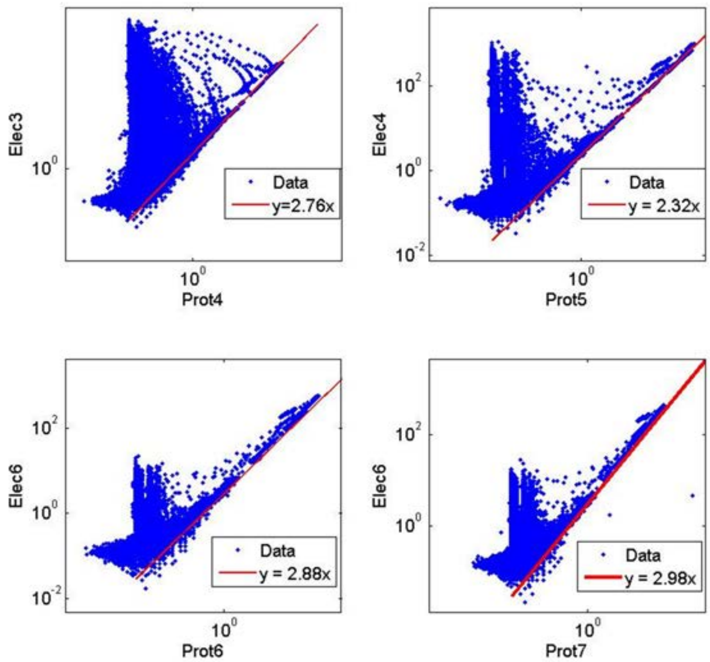

Figure 2. Determination of proton background from scatter plot of channel count rates

3.2. Data Cleaning

The purpose of data cleaning is to identify and eliminate data points with obvious contamination or other problems which would make the data inaccurate. Data cleaning for HEO-1/DOS electrons included the following procedures:

- As previously mentioned appropriate proton channels were used to estimate the proton background
- An SPE flag based on GOES proton data was used to remove data during solar proton events
- Time-offset scatter plots. These plots would ordinarily reveal anomalous spikes in the time series data. Virtually no spikes were identified, but a filter was implemented to catch the few spikes that existed.
- Count histograms. These plots can identify potential pile-up or dead-time issues; none were found.
- Data was not used in the model for $\log_{10}(\Phi) \leq -0.6$.

HEO-3/Dosimeter Electrons

1. Spacecraft

The HEO-3 satellite is in a highly elliptical orbit with period of about 12 hours, perigee of about 500 km, apogee of about 39000 km, and inclination of about 63°. This type of orbit covers the inner zone, slot region and the outer zone of the radiation belts. Data used for AE9 covered from November 1997 to February 2011.

2. Detector

The satellite database of flux data consist of energetic particle measurements, which are 15-second averages of particle data collected in 1-second integration intervals from the various on-board sensors. The E4/Elec4 channel (>0.63 MeV) was not used.

Table 1. Characteristics of HEO-3/DOS channels

Channel	E (MeV)	G (cm^2 sr)	Cosmic Ray BG (cts/sec)	Proton Background (channel & coefficient)
E3/cElec3	>0.45	0.46	0.010	1.78*Prot4
E5/cElec5	>1.5	0.45	0.012	2.41*Prot6
E6/cElec6	>3.0	0.45	0.013	2.05*Prot7

2.1. Response Functions

The HEO-3/DOS channels respond to a rather broad range of energies starting at approximately the threshold level. Because of this, calibrated channel responses were used as a function of incident particle energy in the spectral inversion algorithm as was done for HEO-1/DOS.

2.4 Background Determination

Background count rates were determined by averaging counts in each channel in regions outside the nominal radiation belts. The proton background coefficients for each electron channel were estimated from scatter plots of the electron versus proton channels in a similar fashion as done for HEO-1/Dios. The resulting background is given in Table 1.

3. Data Processing

This section briefly describes the procedures to go from count rates to the calibrated differential directional fluxes used to develop AE9. The details of these procedures will be documented elsewhere.

3.1. Data Formatting and Filtering

The data was first summed into 0.1 wide L-bins for each orbit before performing the subsequent filtering and inversion steps. The background counts were then determined for each L-bin interval and the proton background was estimated using the appropriate proton channel and coefficient. If the count rates in each channel were higher than the background and no solar proton event was present during the period of measurement then a spectral inversion similar to the CEASE TSX-5 instrument was performed.

3.2. Data Cleaning

The purpose of data cleaning is to identify and eliminate data points with obvious contamination or other problems which would make the data inaccurate. Data cleaning for HEO-3/DOS electrons included the following procedures:

- As previously mentioned appropriate proton channels were used to estimate the proton background
- An SPE flag based on GOES proton data was used to remove data during solar proton events
- Time-offset scatter plots. These plots would ordinarily reveal anomalous spikes in the time series data. Virtually no spikes were identified, but a filter was implemented to catch the few spikes that existed.
- Count histograms. These plots can identify potential pile-up or dead-time issues; none were found.
- Data was not used in the model for $\log_{10}(\Phi) \leq -0.75$ or for $h_{min} \leq 1100$ km.

HEO-3 electron channel data were adjusted based on comparisons with dose rates from the associated dosimeters.

ICO/Dosimeter Electrons

1. Spacecraft

The ICO satellite is in a 45° inclination near-circular orbit at 10400 km altitude. The orbit covers the slot region and outer zone of the radiation belts. Available data covers from June 2001 to December 2009.

2. Detector

The satellite database consists of energetic particle measurements, which are reported in 130 second intervals. A description of the electron channels and their background count rates is given in Table 1.

Table 1. Characteristics of ICO/DOS channels

Channel	Eth MeV	G cm^2 sr	Cosmic Ray BG cts/sec	Proton Background (channel & coefficient)
Elec1	0.95	0.061	Not estimated*	2.89*Prot1
Elec2	1.97	0.064	0.0080	2.31*Prot2
Elec3	3.52	0.43	0.0098	3.01*Prot3
Elec4	5.45	0.44	0.0110	2.76*Prot4
Elec5	6.75	0.36	0.0130	2.56*Prot5

* No cosmic ray background was used in inversion process

2.1. Response Functions

The ICO/DOS channels respond to a broad range of electron energies and the calibrated response curves were used to extract the measured flux. Figure 1 shows a typical response curve for channel Elec1.

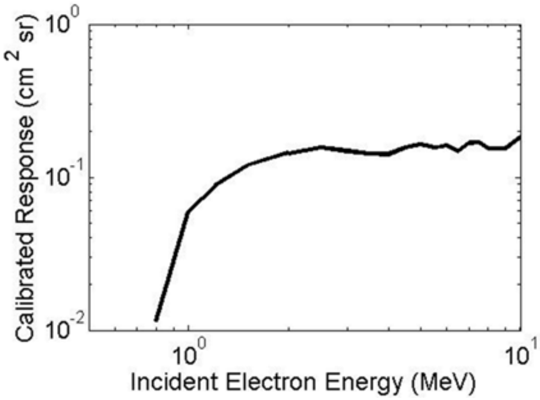

Figure 1. Response of channel Elec3 to isotropic fluxes of electrons

2.5 Background Determination

Background count rates were determined by averaging counts in each channel in regions outside the nominal radiation belts. The proton background coefficients for each electron channel were estimated from scatter plots of the electron versus proton channels in a similar fashion as done for HEO-1/DOS. The resulting background is given in Table 1.

3. Data Processing

This section briefly describes the procedures to go from count rates to the calibrated differential directional fluxes used to develop AE9.

3.1. Data Formatting and Filtering

The background counts were determined for each measurement and the proton background was estimated using the appropriate proton channel and coefficient. If the count rates in each channel were higher than the background and no solar proton event was present during the period of measurement then a spectral inversion similar to the CEASE TSX-5 instrument was performed. Details about the spectral inversion can be found in the CEASE TSX-5 data description.

3.2. Data Cleaning

The purpose of data cleaning is to identify and eliminate data points with obvious contamination or other problems which would make the data inaccurate. Data cleaning for ICO/DOS electrons included the following procedures:

- As previously mentioned appropriate proton channels were used to estimate the proton background
- An SPE flag based on GOES proton data was used to remove data during solar proton events

- Time-offset scatter plots. These plots would ordinarily reveal anomalous spikes in the time series data. Virtually no spikes were identified, but a filter was implemented to catch the few spikes that existed.
- Count histograms. These plots can identify potential pile-up or dead-time issues; none were found.

Polar/HIST Electrons

1. Spacecraft

NASA's Polar satellite was launched in 24 February 1996. The highly elliptical orbit (2 x 9 R_E) had an 85.9° inclination and 17.5 hour period.

2. Detector

The HIST sensor within the CEPPAD package measures both energetic protons and electrons. It includes two Si solid state detectors in front of a plastic scintillator. They measure electrons arriving through a collimator with a 26° full opening angle. The satellite spins with a 6 s period and the data are collected in 16 sectors per spin of 22.5° each. The spin axis is oriented approximately perpendicular to the local magnetic field so that the 16 sectors provide nearly complete pitch angle coverage. Data were collected in 16 energy channels. The energy range each channel varied due to mode cycling designed to reduce measurement errors in different operating environments. Details of the instrument and its operation are given in reference [1].

3. Data Processing

The data processing methods and the final data set adopted for AE9 are described in references [2] and [3]. There are 6.4-minute averages of differential electron intensity at seven kinetic energies from 0.8 to 6.4 MeV, with approximately logarithmic spacing. Energies were 0.8, 1.1, 1.6, 2.2, 3.2, 4.5, and 6.4 MeV. Only angular sectors closest to perpendicular to the local measured magnetic field were selected. Energy response functions for each channel were adapted to a "bow-tie" analysis method and, for consistency across mode changes, resulting energy spectra were then interpolated to the selected energies of the reduced data set. This data set comprised 137,753 observations.

4. Data cleaning

Polar HIST electron observations are affected by saturation at high fluxes (~$2x10^5$ $s^{-1}cm^{-2}sr^{-1}$) and by background/noise contamination at low fluxes (~5 $s^{-1}cm^{-2}sr^{-1}$). Sample plots of Polar HIST electron observations vs. L* are shown in Figure 1. The saturation was noted in cross-calibration conjunction analysis with GPS NS24 which suggested the HIST electron response tended to roll-over above ~$2x10^5$ $s^{-1}cm^{-2}sr^{-1}$ (i.e. as with a paralyzing dead time issue). As used in AE9, each dataset is binned in the standard K-Φ bins and the median and 95th percentile in each bin are obtained to describe the distribution. Consequently, we rejected data from a given bin if either (1) the median is below the background/noise floor or (2) the 95th percentile is affected by saturation. Figure 2 shows plots of K-Φ bins rejected on this basis for two energies. After applying these criteria, about 70,000 usable observations remained for the 0.8-3.2 MeV channels each, 49,800 for the 4.5 MeV channel, and 19,000 for the 6.4 MeV channel.

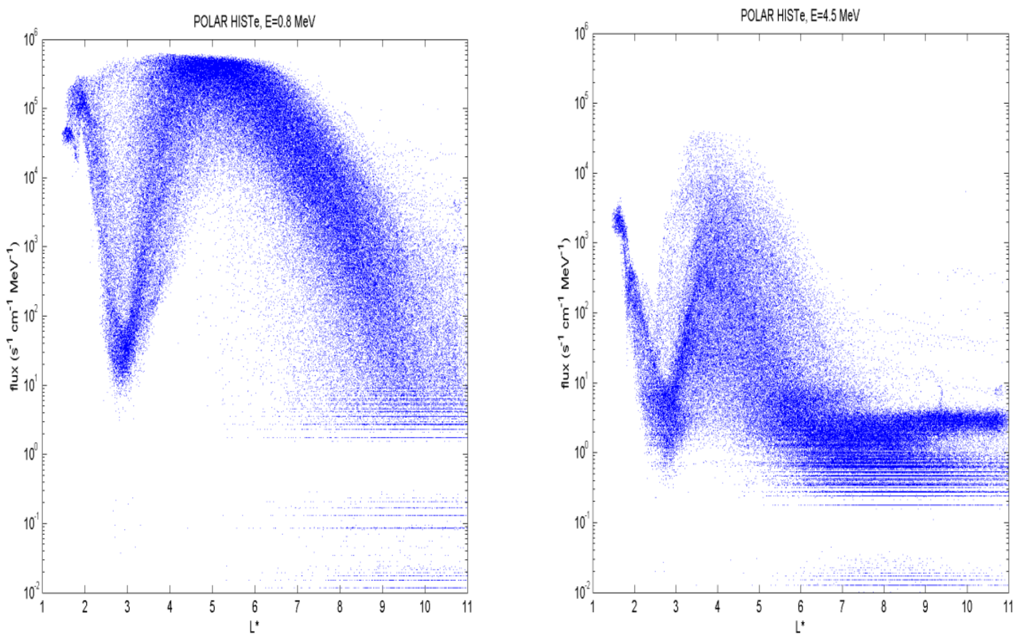

Figure 1: Polar HISTe fluxes vs. L* for energies of 0.8 MeV and 4.5 MeV.

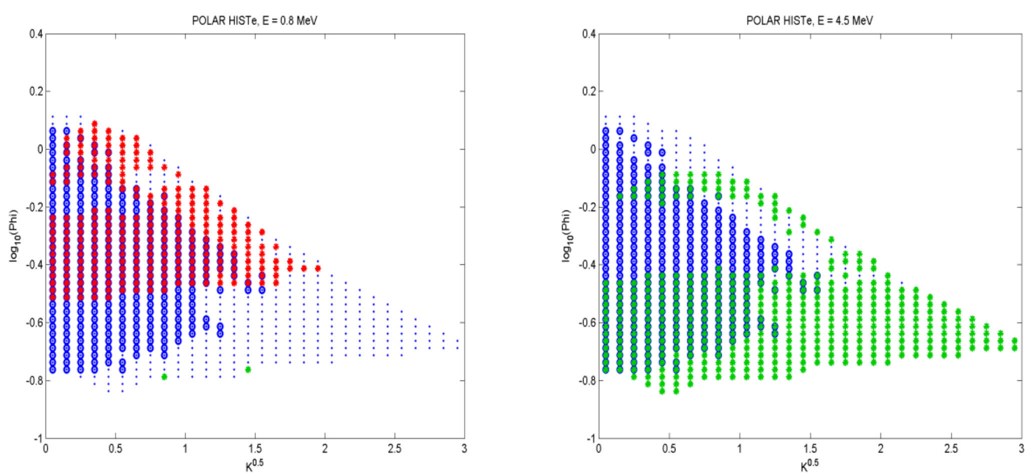

Figure 2: K-Φ bins with Polar HISTe data, for 0.8 MeV and 4.5 MeV. Blue points indicate bins with HISTe data, blue circles those with at least 100 observations. Red indicates bins rejected due to saturation at the 95^{th} percentile or below; green indicates bins rejected due to background/noise at the median or above.

5. References

[1] Blake, J. B., et al., *Space Sc. Rev.*, 71, 531, 1995.
[2] Selesnick and Blake, *J. Geophys. Res.*, 105, 2607, 2000.
[3] Selesnick and Blake, *J. Geophys. Res.*, 107, 1265, 2002.

SAMPEX/PET Electrons

1. Spacecraft

NASA's Solar, Anomalous, and Magnetospheric Particle Explorer (SAMPEX) satellite was launched 3 July 1992. The orbit had an 82° inclination and an altitude of 520-670 km. The satellite is still operational, although the NASA science mission (and hence NSSDC-available data) ended 30 June 2004.

2. Detector

The Proton/Electron Telescope consists of twelve 2- to 3-mm thick silicon solid-state detectors grouped into eight functional units to form a multi-element telescope. Through a combination of range information in the stack and pulse-height information from the first three detectors, PET distinguishes protons, alphas, and electrons cleanly from one another. Pulse-height information is telemetered for only a sample of particles entering the telescope. It has approximately 60° field-of-view and geometric factor of 1-10 cm^2sr. Details are in reference [1].

3. Data Processing

Electron differential intensity spectra were computed for the energy range 0.5 to 5 MeV using rate data from the front P1 detector and pulse-height analyzed event data from the ELO and EHI data types. Spectra were calculated for data accumulated over consecutive 30 s intervals each day. The model spectrum is made up of 11 continuous, piecewise exponential segments. Data were simulated using calibrated response functions, assuming an isotropic distribution, and a least-squares fit including a smoothness assumption to prevent fluctuations from noisy data. Corrections were made for deadtime using the PET livetime counter and for chance coincidences in ELO using the P1 and P2 single detector response functions. Livetime from each 6-s rate accumulation weighted the counts from that interval. Data were restricted to $2<L<8$ (there was significant proton contamination for $L<2$). IGRF L values from the SAMPEX data sets were used. The analysis procedure was based on one developed originally for solar electrons and described in reference [2]. Extracted energies were 0.500, 0.909, 1.318, 1.727, 2.136, 2.546, 2.954, 3.364, 3.773, 4.182, 4.591, and 5.000 MeV. Data processed for AE9 covers from 1993 to 2004.

4. Data cleaning

Given the wide angular response of PET, only observations corresponding to a pitch angle greater than 45° were used. The data set was also narrowed to observations with valid invariant magnetic coordinates and not during SPEs. A small fraction of inversions yielded flat spectra (i.e. identical fluxes at all energies) which were rejected. Some inversions yielded straight power law spectra; scatter plots of successive channel fluxes in these cases showed distributions significantly at variance with similar comparisons from CRRES MEA and HEEF data.

Therefore these observations were also omitted from further use. This left 328,131 observations with K-Φ coordinates, or 363,494 observations with K-Hmin coordinates.

SAMPEX PET electron observations are affected by saturation at high fluxes and by background/noise contamination at low fluxes, as illustrated in Figure 1. As used in AE9, each dataset is binned in the standard K-Φ (and likewise for K-Hmin) bins and the median and 95th percentile in each bin are obtained to describe the distribution. Consequently, we reject data from a given bin if either (1) the median is below the background/noise floor or (2) the 95th percentile is affected by saturation. Few observations were left at 0.5-1.3 MeV or at 4.18-5.00 MeV, so these channels were not used. For the remaining six channels, 89,000 to 106,000 usable observations were left at 1.73 to 2.95 MeV, ~60,000 at 3.36 MeV, and ~10,000 at 3.77 MeV.

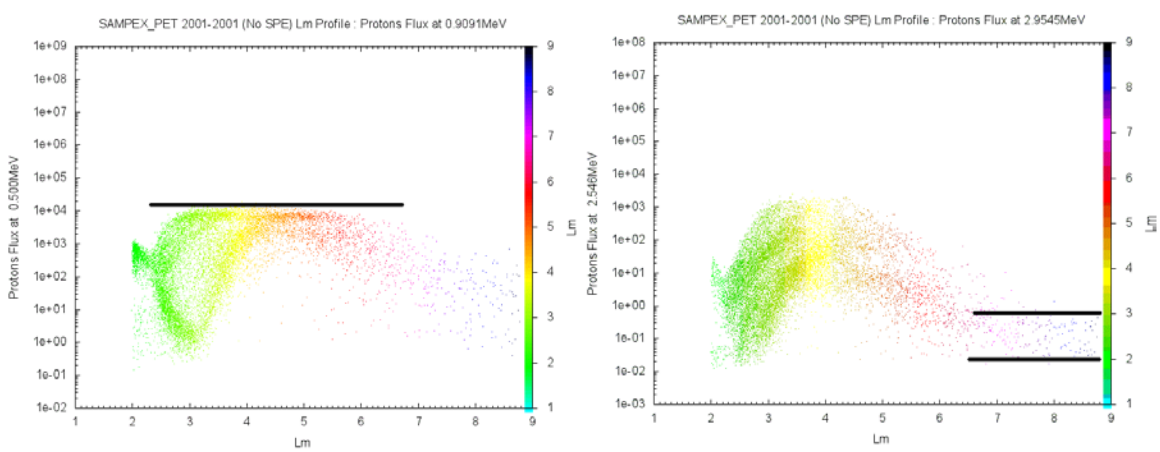

Figure 1: PET electron fluxes vs. Lm for two channels, illustrating the high flux saturation limit in the 0.909 MeV channel (left) and the low flux noise/background limit in the 2.954 MeV channel (right).

5. References

[1] Cook et al., *IEEE Trans. Geoscience Remote Sensing*, 31, 565, 1993.
[2] Mewaldt et al., *J. Geophys. Res.*, 110, A09S18, 2005.

SCATHA/SC3 Electrons

1. Spacecraft

As a joint Air Force/NASA satellite mission, the Spacecraft Charging AT High Altitudes (SCATHA) was launched on 30 January 1979 as into a highly elliptical transfer orbit having an apogee of 43,183km, a perigee of 176 km, and an inclination of 27.3°. On February 2, 1979, SCATHA was inserted into its final, near-synchronous Earth orbit at 7.9° inclination with apogee at 43,192 km (~7.8 R_E), perigee at 27,517 km (~ 5.3 R_E), and period of 23.597 hours [1][2]. This mission lasted about 11 years.

2. Detector

The SC3 spectrometer on board SCATHA measured the fluxes and pitch-angle (PA) distributions of energetic electrons in the energy range 47 keV to 5 MeV. Information on the 24 energy channels is listed in Table 1 [1]. The center energy is in the unit of keV, while the geometric factor term $(G_F\Delta E)^{-1}$ is in units of cm^{-2} sr^{-1} keV^{-1}.

Table 1: Information for the 24 energy channels of SCATHA/SC3.

Low Energy Mode				High Energy Mode			
Center E (keV)	Energy range (keV)	ΔE (keV)	$(G_F\Delta E)^{-1}$ (cm^{-2} sr^{-1} keV^{-1})	Center E (keV)	Energy range (keV)	ΔE (keV)	$(G_F\Delta E)^{-1}$ (cm^{-2} sr^{-1} keV^{-1})
56.7	47-66	19	19.9	448.5	260-630	370	1.74
76.7	66-87	21	18.7	830	630-1030	400	1.05
97.5	87-108	21	18.3	1222.5	1030-1420	390	1.08
118.5	108-129	21	18.3	1616.5	1420-1810	390	1.14
139.5	129-150	21	18.3	2011	1810-2210	400	1.22
160.5	150-171	21	18.3	2405.5	2210-2600	390	1.26
181.5	171-192	21	18.6	2800	2600-3000	400	1.38
203	192-214	22	17.9	3195	3000-3390	390	1.48
224.5	214-235	21	19.5	3590	3390-3790	400	1.80
245.5	235-256	21	22.2	3904	3790-4180	390	2.14
267	256-278	22	25.5	4378	4180-4580	400	3.25
288.5	278-299	21	32.9	4772.5	4580-4970	390	3.68

3. Data Processing

The SCATHA data were recovered in late 1990s by the Aerospace Corporation and a different table of geometric factor parameters was provided by [3]. However, the geometric factors by Fennel et al. are only available for 12 low energy channels; hence, we have chosen to adopt parameters provided by [1] to convert count rates to differential energy fluxes (j) with an equation

$$j = \text{counts}/(\Delta t\ G_F\ \Delta E)$$

for both low and high energy channels.

The electron count rate data used in AE9/AP9 were extracted from high-resolution Common Data Format (CDF) files provided by the Aerospace Corporation. The original time resolution of the SC3 data is 0.496 sec. In order to reduce the SCATHA/SC3 dataset to a manageable size, measured count rates have been averaged over 5-min intervals in 9 local pitch angle bins from 0° to 90°. Each pitch angle bin has a resolution of 10°.

The SCATHA satellite ephemeris information contained in the associated "summary CDF" files was determined to be very poor quality and contained many unphysical position shifts. A database of SCATHA satellite orbit two-line element (TLE) sets was obtained from the Aerospace Corporation. The 'Lokangle' propagator was used to generate a replacement set of ephemeris information from a filtered version of this TLE database; many TLE entries that were deemed suspicious, or those that caused unphysical position shifts, were removed.

4. Data cleaning

Three types of data cleaning processes were performed (1) to correlate count rates from neighboring energy channels (Fig. 1a-b); (2) to plot count rates for one energy channel against itself at a 5-min time lag (Fig. 1c); and (3) to use the median values to filter out spurious high count rates. Examples of cleaning methods are shown in Figure 1. Suspicious points outside a selected diagonal range marked by two black lines (Fig. 1a and 1c) were flagged and were not included in the product. Energy channel 13 did not function properly after the first two years of operation as seen in Figure 1b, hence, data from this energy channel (highlighted red in Table 1) has been excluded in the product.

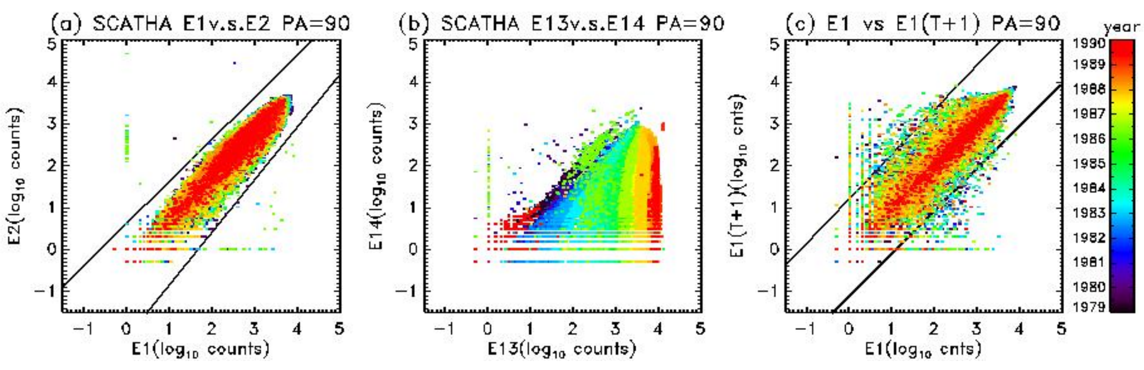

Figure 1. (a) Correlation between two adjacent energy channels, 1 and 2, for pitch angles 80°-90°. Data points outside the two diagonal solid black lines were excluded in our statistical study. The color bar on the right of each panel indicates the year of mission. (b) Correlation between energy channels 13 and 14. This panel and other information (not shown) indicate that the energy channel 13 does not provide accurate count rate measurements for the majority period of the mission. (c) A plot of energy channel 1 against itself at a 5-min time lag. Again, data points above the upper black line and below the lower line were excluded in our statistics.

Finally, electron fluxes of 23 energy channels with time and pitch angle resolution of 5 min and 10° [i.e., j(nE=23, nPA=9, Δt=5 min)] along with corresponding L_m, K, ϕ, and HMIN were generated to be used in the AE9/AP9 product.

5. References

[1] Reagan, J. B., R. W. Nightingale, E. E. Gaines, W. L. Imhof, and E. G. Stassinopoulos (1981), Outer zone energetic electron spectral measurements, *Proceedings of the AIAA 18th Aerospace Sciences Meeting*, AIAA-80 0390, Pasadena, CA.

[2] Fennell, J. F. (1982), Description of P78-2 (SCATHA) satellite and experiments, in the *IMS Source Book*, Russell and Southwood Ed., 65-81, American Geophysical Union, Washington, D.C.

[3] Fennell, J. F., G. M. Boyd, M. T. Redding, and M. C. McNab (1997), Data recovery from SCATHA satellite, Aerospace Report No. ATR-97(7400)-1.